

Yang-Lee edge singularities at high temperatures

Douglas A. Kurtze and Michael E. Fisher

Baker Laboratory, Cornell University, Ithaca, New York 14853

(Received 26 April 1979)

The density of Lee-Yang zeros, in the thermodynamic limit, for classical n -vector models and for the quantum Heisenberg model is studied in the asymptotic high-temperature limit. It is shown that the high-temperature series expansions for these models reduce, in this limit, to the corresponding low-density expansions for the monomer-dimer problem with negative dimer activity. If the density of zeros, $g(h'')$, on the imaginary axis of the complex reduced-magnetic-field plane, $h = H/k_B T = h' + ih''$, has an algebraic singularity at the edge of the gap in the zero distribution, $g(h'') \sim [|h''| - h_0(T)]^\sigma$, then σ is independent of n in this limit. Analyzing dimer density series on various lattices by means of the ratio test, Dlog Padé, the recursion-relation method, and inhomogeneous differential approximants, we obtain the estimates $\sigma = -0.163 \pm 3$ for $d=2$ dimensions and $\sigma = 0.086 \pm 15$ for $d=3$.

I. INTRODUCTION

Although the concept of zeros of the partition function¹ has been employed in proofs of the absence of phase transitions in certain systems, little is known about the actual form of the density of zeros in the thermodynamic limit and its relation to observable behavior. In the present work we address this problem by investigating the singularities in the zero density which occur at the edge of the distribution of zeros in the complex magnetic-field plane for classical n -vector models and for the quantum Heisenberg model in the asymptotic limit of high temperatures. These singularities, which represent the zeros lying closest to real values of the field, should exert the greatest influence on real physical behavior. We establish analytically that the nature of these singularities is independent of the symmetry number, n , of the spins in the model for a wide class of Hamiltonians, and numerically estimate the exponents characterizing them for models with ferromagnetic nearest-neighbor interactions on lattices of spatial dimensionalities $d=2$ and 3.

The relation of the distribution of Lee-Yang zeros to the occurrence of phase transitions is conveniently illustrated by the ferromagnetic Ising model. If the partition function of this model is viewed as a function of complex magnetic field, H , then for real temperature T its zeros are known² to be confined to the imaginary field axis (although with antiferromagnetic interactions present, the location of the zeros is not known rigorously). Yang and Lee argued¹ that for a system above its critical temperature T_c , whose free energy is an analytic function of the real field, the partition function must be nonzero throughout some neighborhood of the real axis in the complex

reduced-magnetic-field plane,

$$h = H/k_B T = h' + ih'' \quad , \quad (1.1)$$

where H is measured in energy units, k_B is Boltzmann's constant, and h' and h'' are, respectively, the real and imaginary parts of h . Below T_c , however, the zeros will come arbitrarily close to the real h axis as the thermodynamic limit is taken, destroying the analyticity of the free energy in H for those real fields at which zeros accumulate. Thus, for temperatures above critical a gap will be found on the imaginary h axis with edges at, say, $\pm ih_0(T)$, which is free of zeros. In fact, the existence of such a gap has been proven³ for sufficiently high temperatures, and Bessis *et al.*⁴ give upper and lower bounds for $h_0(T)$. If we define a density of zeros, $g(h'')$, in such a way that as N , the number of spins in the system, becomes infinite, the quantity $Ng(h'') dh''$ approaches the number of zeros between ih'' and $i(h'' + dh'')$ on the imaginary h axis, then $g(h'')$ will vanish for $|h''| < h_0(T)$. Since nonanalytic behavior must set in at T_c , the size of the gap must vanish when $T = T_c$.

Kortman and Griffiths⁵ first pointed out the interest of investigating the behavior of $g(h'')$ near $\pm h_0(T)$. By analyzing high-field and high-temperature series for ferromagnetic Ising models on the square and tetrahedral lattices, they concluded that the density of zeros near the edges of the gap exhibits a power-law behavior

$$g(h'') \sim [|h''| - h_0(T)]^\sigma \quad , \quad \text{for } |h''| \rightarrow h_0(T) + \quad (1.2)$$

The estimates of the exponent σ showed little variation with temperature for $T \geq 3T_c$, and it was proposed that σ should be independent of T for $T > T_c$,

taking the values $\sigma = -0.125 \pm 50$ for the square lattice and $\sigma = +0.125 \pm 50$ for the tetrahedral lattice.

In the present work, we focus our attention on σ . Since the Yang-Lee edge bears a strong resemblance to an ordinary critical point,⁶ one would expect σ to depend not on the detailed lattice structure of the model but only on its dimensionality d and symmetry number n . However, we will further demonstrate explicitly that, in the high-temperature limit, σ is independent of n ($< \infty$), and also of the form of the interactions between spins. The results of Kortman and Griffiths, as well as exact solutions for the one-dimensional nearest-neighbor Ising model,² the mean field model,⁵ and the spherical model,⁷ indicate that the value of σ for any model should be the same for all $T > T_c$. Thus we expect to find σ independent of n for all temperatures above critical. Accordingly, we refine Kortman and Griffiths' estimates of σ by analyzing series expansions for Ising models in the high-temperature limit, which reduce^{6,8} to those for the monomer-dimer problem⁹ on the same lattice. We use longer series¹⁰ and more powerful methods of analysis¹¹⁻¹³ than were available to Kortman and Griffiths, and study series, not only for the square and tetrahedral lattices, but also for the triangular, simple cubic (sc), bcc, and fcc lattices.

In Sec. II, we recall the connection between the magnetization of a model and its Lee-Yang zero distribution. Section III demonstrates the reduction of Ising-model series to the corresponding monomer-dimer series in the high-temperature limit,^{6,8} while Sec. IV shows that these series also represent the high-temperature limit of series for classical n -vector models with general nearest-neighbor interactions and for the quantum Heisenberg model. Our series analysis and final estimates of σ for $d=2$ and 3 are presented in Sec. V, and the results are discussed in Sec. VI.

II. ELECTROSTATIC ANALOGY

In the models we consider, we take the zeros of the partition function to lie on the imaginary h axis, which is known rigorously to be the case for ferromagnetic quantum^{14,15} and classical¹⁶ XY and Heisenberg models. Although the corresponding theorem for classical ferromagnetic n -vector models with $n > 3$ is not yet available, both renormalization group⁶ and numerical¹⁷ analyses support this view. The zero distribution of such a model, $g(h'')$, is accessible from its thermodynamic equation of state by means of the electrostatic analogy expounded by Lee and Yang.² This approach rests on the observation that the free energy of the model can be written

$$F(T, H) = -k_B T \int g(h'') \ln(h - ih'') dh'' \quad (2.1)$$

with h'' running between appropriate limits. The

form of the free energy is exactly the same as that of the two-dimensional electrostatic potential due to a line charge of density $g(h'')$ located along the imaginary h axis; this fact gives the method its name. The reduced magnetization, analogous to the electric field, is then given by

$$M = -\frac{1}{k_B T} \left(\frac{\partial F}{\partial h} \right)_T = \int \frac{g(h'') dh''}{h - ih''} \quad (2.2)$$

Now the thermodynamic equation of state defining the function $M(h)$, when written in this form, can readily be continued analytically to give M as a function of complex h . Mathematically, the right-hand side of (2.2) is closely related¹⁸ to a Cauchy integral. By applying this fact, which is equivalent to using Gauss' law in the electrostatic interpretation, one finds that the discontinuity in $M(h)$ as one crosses the locus of zeros at ih'' from left to right is just $2\pi g(h'')$. Thus in order to extract the zero density $g(h'')$ for these models, one merely reads off the discontinuity in $M(h)$ at $h = ih''$.

The edges of the locus of zeros stand identified as branch points of $M(h)$; if, near these edges, $M(h)$ displays the branch point behavior

$$M(h) \sim [h \pm ih_0(T)]^\sigma \quad (2.3)$$

then the zero density $g(h'')$ will have the asymptotic form

$$g(h'') \sim [|h''| - h_0(T)]^\sigma, \quad \text{for } |h''| \rightarrow h_0(T) + , \\ = 0, \quad \text{for } |h''| < h_0(T) \quad (2.4)$$

At the critical temperature, however, one expects¹⁹ to find

$$M(h) \sim h^{1/\delta} \quad (2.5)$$

so for $T = T_c$, σ is equal to the standard exponent $1/\delta$ which describes the real critical isotherm.

III. HIGH-TEMPERATURE SERIES FOR ISING MODELS

In order to analyze the singularity (2.3) we will examine the high-temperature series expansions for $M(h)$ in the models under consideration. First, however, we outline the well-known development of these series for Ising models. Baker and Moussa⁸ and Fisher⁶ observed independently that for high temperatures the Ising magnetization series reduces to the dimer density series in the monomer-dimer problem; we present the derivation here in order to illustrate those features which will lead to a similar reduction in other models.

The Ising model consists of N spin variables which can take on only the values ± 1 , associated with the N

sites R_i of a regular lattice; the total spin Hamiltonian is

$$\mathcal{H} = -J \sum_{\langle ij \rangle} s_i s_j - H \sum_i s_i \quad (3.1)$$

The first summation on the right-hand side runs over pairs (i, j) such that R_i and R_j are nearest-neighbor lattice sites. If the exchange coupling J is taken to be positive, the system is ferromagnetic. The partition function is given by

$$Z_N(T, H) = \sum_{\{s_i\}} \exp \left(K \sum_{\langle ij \rangle} s_i s_j + h \sum_i s_i \right) \quad (3.2)$$

where

$$K = J/k_B T, \quad h = H/k_B T \quad (3.3)$$

and the outer summation runs over all possible sets of values of the spin s_i . The binary nature of the spins easily yields the relations

$$\exp(Ks_i s_j) = \cosh K (1 + v s_i s_j) \quad (3.4)$$

with $v = \tanh K$

$$\exp(hs_i) = \cosh h (1 + \tau s_i) \quad (3.5)$$

with $\tau = \tanh h$

so that v and τ are small for small K and h , respectively. If the lattice has coordination number q , Eq. (3.2) then becomes

$$Z_N(T, H) = (\cosh K)^{Nq/2} (\cosh h)^N \times \sum_{\{s_i\}} \left(\prod_{\langle ij \rangle} (1 + v s_i s_j) \right) \left(\prod_i (1 + \tau s_i) \right) \quad (3.6)$$

By multiplying out the products and summing over spin configurations we arrive at an expansion of Z_N in powers of v and τ .

Each term in the expansion of the products in Eq. (3.6) can be represented by a graph^{19,20} drawn on the lattice, with each factor of $v s_i s_j$ represented by the corresponding bond and each τs_i by the corresponding vertex. A graph in which any spin s_k occurs an *odd* number of times gives no contribution, since the sum over s_k gives zero. Thus only even powers of τ appear in the expansion of Z_N , reflecting the symmetry of the system with respect to reversal of the magnetic field. This fact also implies that no terms involving $v^k \tau^{2l}$ with $l > k$ can contribute, since any graph of k distinct bonds and $2l > 2k$ distinct magnetic vertices must have isolated vertices. In addition, since $s_i^2 = 1$ holds identically, the sum over spin configurations in the remaining terms is trivial, reducing to multiplication by 2^N . Taking the logarithm of Eq. (3.6) and passing to the thermodynamic

limit then yields the form

$$F(T, H) = -k_B T \left(\ln 2 \cosh h + \frac{1}{2} q \ln \cosh K + \sum_{l=1}^{\infty} l^{-1} v^l \sum_{m=0}^l \psi_{lm} \tau^{2m} \right) \quad (3.7)$$

for the free energy per spin, with the constants ψ_{lm} determined from the number of embeddings²⁰ of graphs of l bonds and $2m$ magnetic vertices in the lattice. The magnetization per spin is given by

$$M(T, H) = \tau + 2(1 - \tau^2) \sum_{l=1}^{\infty} l^{-1} v^l \sum_{m=1}^l m \psi_{lm} \tau^{2m-1} \quad (3.8)$$

Passing to the high-temperature limit will reduce our problem from analyzing a series in two variables to analyzing a single-variable series. In order to retain a magnetic field dependence in M , we must take this limit in such a way that the quantity

$$z = v\tau^2 = (\tanh h)^2 \tanh K \quad (3.9)$$

approaches a finite limit as $v \rightarrow 0$. In this limit, the magnetization is given by

$$M(T \rightarrow \infty, h) = \tau [1 - 2\rho(z)] \quad (3.10)$$

with

$$\rho(z) = \sum_{l=1}^{\infty} \psi_{ll} z^l \quad (3.11)$$

If, as expected, $M(T \rightarrow \infty, h)$ behaves according to Eq. (2.3) near its singularities at $\pm ih_0(T \rightarrow \infty)$, then clearly $\rho(z)$ must obey

$$\rho(z) \sim (z + z_0)^\sigma \quad (3.12)$$

for z near $-z_0$, where

$$z_0 = \lim_{T \rightarrow \infty} \tan^2[h_0(T)] \tanh K \quad (3.13)$$

The existence of z_0 implies that $h_0(T)$ is given asymptotically by

$$h_0(T) \approx \frac{1}{2} \pi - (J/z_0 k_B T)^{1/2} + O(T^{-3/2}) \quad (3.14)$$

for high temperatures. For $J > 0$, zeros of the partition function occur only at purely imaginary values of h , so z_0 must be real and positive.

Since no $v^l \tau^{2m}$ terms with $m > l$ can occur in $Z_N(T, H)$, the z^l terms in the magnetization can arise only from $v^l \tau^{2l}$ terms in the partition function, which correspond to graphs of l bonds and $2l$ magnetic vertices. The only contributing graphs of this type consist of l *separated* bonds with magnetic vertices at their end points, since if any two bonds shared an end point, some magnetic vertex would necessarily be isolated and the weight of the graph would be zero. These l bonds, then, behave exactly as hard di-

mers, and so the coefficient of z^l in $Z_N(T \rightarrow \infty, H)$ is simply the number of ways of placing l hard dimers on the lattice.⁹ In other words, as $T \rightarrow \infty$, $Z_N(T, H)$ becomes the partition function for ideal hard dimers on the lattice with dimer activity z , and $\rho(z)$ is then the dimer density series.⁹

IV. HIGH-TEMPERATURE SERIES FOR n -VECTOR MODELS

The development of high-temperature series expansions for classical n -vector models parallels the Ising analysis quite closely. We will consider a model in which the sites of a lattice are occupied by n -dimensional unit vector spins which interact through the general nearest-neighbor potential $nJ\varphi(\vec{s}_i, \vec{s}_j)$. With a magnetic field of strength $nH = nk_B T h$ applied in the \hat{z} direction, the partition function for n spins on the lattice is

$$Z_N(T, H) = c_n^{-N} \int d^N \Omega \exp \left(nK \sum_{\langle ij \rangle} \varphi(\vec{s}_i, \vec{s}_j) + nh \sum_i s_i^z \right), \quad (4.1)$$

$$Z_N(T, H) = f^N c_n^{-N} \int d^N \Omega \prod_{\langle ij \rangle} [1 + v(\vec{s}_i, \vec{s}_j; K)] \prod_i [1 + \tau(\vec{s}_i; h)], \quad (4.4)$$

where now we have

$$v(\vec{s}_i, \vec{s}_j; K) = \left(\exp[nK\varphi(\vec{s}_i, \vec{s}_j)] / c_n^{-2} \int d\Omega \int d\Omega' \exp[nK\varphi(\vec{s}, \vec{s}')] \right) - 1, \quad (4.5)$$

$$\tau(\vec{s}_i; h) = \left(\exp[nhs_i^z] / c_n^{-1} \int d\Omega \exp[nhs^z] \right) - 1 = [(\frac{1}{2}nh)^{n/2-1} \exp(nhs_i^z) / \Gamma(\frac{1}{2}n) I_{n/2-1}(nh)] - 1, \quad (4.6)$$

with $I_\nu(x)$ denoting the usual modified Bessel function, and

$$f = \left(c_n^{-2} \int d\Omega \int d\Omega' \exp[nK\varphi(\vec{s}, \vec{s}')] \right)^{q/2} c_n^{-1} \int d\Omega \exp[nhs^z]. \quad (4.7)$$

The functions $v(\vec{s}_i, \vec{s}_j; K)$ and $\tau(\vec{s}_i; h)$ vanish linearly as K and h go to zero respectively, and also yield zero when integrated over their spin arguments; they play the same roles as $v_{s_i s_j}$ and τ_{s_i} in the Ising model. By multiplying out the products in Eq. (4.4) and performing the required integrations one obtains, as in the Ising case, an expansion in graphs having no multiple bonds or repeated magnetic vertices. The weight attached to each graph is calculated by writing a factor $v(\vec{s}_i, \vec{s}_j; K)$ for each line in the graph and $\tau(\vec{s}_i; h)$ for each magnetic vertex, and then integrating over all spins. Since $\tau(\vec{s}_i; h)$ by itself integrates to zero, no graphs containing isolated magnetic vertices can contribute to $Z_N(T, H)$. This is the feature crucial to the emergence of the monomer-dimer series at high temperatures: any contributing graph with l bonds and m magnetic vertices must satisfy $m \leq 2l$, with equality attained only in graphs consist-

where the integral runs over the surface of each unit n sphere, and

$$c_n = \int d\Omega = \frac{2\pi^{n/2}}{\Gamma(\frac{1}{2}n)}. \quad (4.2)$$

The factors of n in the exponent ensure that the free energy per spin component,

$$F(T, H) = -k_B T \lim_{N \rightarrow \infty} (nN)^{-1} \ln Z_N(T, H), \quad (4.3)$$

continues to exist in the spherical model limit $n \rightarrow \infty$.^{21,22} Taking $n=1$ reproduces the Ising model, but with a generalized spin-spin interaction. Note that $\varphi(\vec{s}, \vec{s}')$ need not be isotropic, and in fact the following analysis is not affected by the presence of a single-spin or "hidden field" term in φ . However, φ must satisfy a condition, to be made explicit below, which excludes the form $\varphi(\vec{s}, \vec{s}') = \varphi_1(\vec{s}) + \varphi_1(\vec{s}')$, so that nontrivial coupling must be present. Furthermore, for a thermodynamically sensible model, φ will have to satisfy certain conditions; for all practical purposes uniform boundedness should suffice.

The partition function (4.1) may be rewritten in the form

ing of l hard dimers. Each l -dimer graph carries a weight z^l , where the "dimer activity" z is now given by

$$z = c_n^{-2} \int d\Omega_1 \int d\Omega_2 \tau(\vec{s}_1; h) v(\vec{s}_1, \vec{s}_2; K) \tau(\vec{s}_2; h). \quad (4.8)$$

We will argue that for high temperatures with z kept finite the weights of all other graphs go to zero.

Consider the argument first for the usual isotropic interaction $\varphi(\vec{s}, \vec{s}') = \vec{s} \cdot \vec{s}'$, for which explicit calculations are possible. In this case, Eq. (4.8) can be evaluated by expanding $v(\vec{s}_1, \vec{s}_2; K)$ and $\tau(\vec{s}_i; h)$ in n -dimensional spherical harmonics,²³ yielding

$$z = \sum_{l=1}^{\infty} \frac{(n+2l-2)(n+l-3)!}{l!(n-2)!} \left[\frac{I_{n/2+l-1}(nh)}{I_{n/2-1}(nh)} \right]^2 \times \frac{I_{n/2+l-1}(nK)}{I_{n/2-1}(nK)}. \quad (4.9)$$

Since $I_\nu(x)$ behaves as $(\frac{1}{2}x)^\nu/\nu!$ for large ν , this series converges for all fixed K and h . For small K it reduces to

$$z = nK [I_{n/2}(nh)/I_{n/2-1}(nh)]^2 + O(K^2) \quad (4.10)$$

As $K \rightarrow 0$, z can approach a finite limit \bar{z} only if the bracketed quantity diverges as $K^{-1/2}$. However, this quantity is the logarithmic derivative of the entire function $x^{1-n/2}I_{n/2-1}(x)$, which forces

$$nh \approx ix_1 - \left(\frac{J_{n/2}(x_1)}{J'_{n/2-1}(x_1)} \right) \left(\frac{nK}{\bar{z}} \right)^{1/2}, \text{ for } K \rightarrow 0 \quad (4.11)$$

where $J_\nu(x)$ is the ordinary Bessel function and ix_1 is the smallest zero of $I_{n/2-1}(x)$. For $n \geq 0$, x_1 must be purely real, so that imaginary values of h correspond to real negative values of \bar{z} . Now if Eq. (4.11) gives the behavior of h , then from Eq. (4.6) one finds that $\tau(\bar{s}_i; h)$ grows as $K^{-1/2}$ for small K , while $\nu(\bar{s}_i, \bar{s}_j; K)$ is of order K ; any graphs consisting of l bonds and $m < 2l$ magnetic vertices will then carry a weight which vanishes as $K^{l-m/2}$. Thus only dimer graphs survive in the high-temperature, finite- z limit as asserted.

The argument for general pair interactions, $\varphi(\bar{s}_i, \bar{s}_j)$, proceeds similarly. For small K one may expand Eq. (4.5) and thence write the dimer activity as

$$z \approx nK \psi(nh)/[I_{n/2-1}(nh)]^2 \quad (4.12)$$

provided the leading amplitude function

$$\psi(nh) = \sum_{l=1}^{\infty} \sum_{l'=1}^{\infty} \binom{n+l-2}{l} \binom{n+l'-2}{l'} \varphi_{ll'} \times I_{n/2+l-1}(nh) I_{n/2+l'-1}(nh) \quad (4.13)$$

does not vanish identically. In this expression $\varphi_{ll'}$ is the coefficient of $Y(l, 0, \dots, 0; \bar{s}) Y(l', 0, \dots, 0; \bar{s}')$ in the expansion of $\varphi(\bar{s}, \bar{s}')$ in n -dimensional spherical harmonics,²³ normalized so that

$$Y(l, 0, \dots, 0; \hat{z}) = \frac{(n+l-2)!}{l!(n-2)!}, \text{ for } n > 2 \quad (4.14)$$

and taking $Y(l; \bar{s}) = \cos l \bar{s} \cdot \hat{z}$ for $n=2$. Note that this differs by a factor of $(n+l-2)/(n-2)$ from the usual normalization. Since $\varphi(\hat{z}, \hat{z})$ is bounded, $\psi(nh)$ is finite for all h ; thus z can approach a finite limit as $K \rightarrow 0$ only if nh approaches a zero, ix_1 , of $I_{n/2-1}(x)$ (for our purposes, the smallest zero is the most important) with corrections of order $K^{1/2}$, and provided $\psi(ix_1)$ is nonzero, or, equivalently,

$$c_n^{-2} \int d\Omega_1 \int d\Omega_2 \varphi(\bar{s}_1, \bar{s}_2) \times \exp[ix_1(s_1^2 + s_2^2)] \neq 0 \quad (4.15)$$

Under these conditions, imaginary values of h again yield real negative values of \bar{z} , and the contributions from all but hard-dimer graphs vanish as $K \rightarrow 0$, as argued above. Note that any "hidden field" term in $\varphi(\bar{s}, \bar{s}')$ could be absorbed into the magnetic field; at high temperatures its contribution would be of order K , and so would not enter into the leading behavior of h .

We see, then, that with an appropriately defined "dimer activity" held fixed, the high-temperature series expansions for classical n -vector models with general nearest-neighbor interactions become identical to those of the standard Ising model in the asymptotic high-temperature limit. In particular, the same analytic structure is manifest in all these models at high temperatures. This analysis breaks down, as it must, in the spherical model ($n \rightarrow \infty$) limit. Using standard asymptotic expansions for the Bessel functions occurring in Eq. (4.9) for the isotropic case, one can see that the dimer activity is given asymptotically by

$$z \approx \exp \left\{ \frac{8nKh^2}{[1 + (1 + 4h^2)^{1/2}]^2 [1 + (1 + 4K^2)^{1/2}]} \right\} - 1 \quad (4.16)$$

so that as $n \rightarrow \infty$, z diverges for $K > 0$ and real $h \neq 0$ while z goes to -1 for $K > 0$ and any imaginary h . Thus the above analysis does not apply in the spherical model limit.⁷

The arguments given here can be generalized to cover further-neighbor pair interactions $nJ\varphi_{ij}(\bar{s}_i, \bar{s}_j)$ and m -body interactions. In the former case, the dimer graphs still dominate as $K \rightarrow 0$, although the various classes of dimers (nearest-neighbor, second-neighbor, etc.) will carry different weights, given by replacing $\varphi(\bar{s}_i, \bar{s}_j)$ by $\varphi_{ij}(\bar{s}_i, \bar{s}_j)$ in the expression (4.5) for $\nu(\bar{s}_i, \bar{s}_j; K)$ and using this in Eq. (4.8). With m -body interactions present, however, the " m -mer" graphs of highest m will dominate at high temperatures. In such a graph, each m -body interaction term, which gives a factor of order K , has associated with it m magnetic vertices, and so has a weight whose small- K behavior is governed by a factor $K [I_{n/2}(nh)/I_{n/2-1}(nh)]^m$ for each m -mer. In order for the m -mer activity to remain finite, it is only necessary to have the bracketed quantity growing as $K^{-1/m}$, and so the weight of, say, a graph of l dimers would vanish as $K^{l(m-2)/m}$.

We also expect that this analysis extends to cover models in which the spin length is a continuous variable, where a weighting term $\exp[-\sum_i W(s_i^2)]$ is included in the partition function to control the fluctuations in spin length. In this case, integrals over the surface of the unit sphere are replaced by integrals over all \bar{s} ; for small K , the dimer graphs will be dom-

inant provided h varies in such a way that

$$\left(\frac{1}{2}nh\right)^{1-n/2} \int_0^\infty s^{n/2} I_{n/2-1}(nhs) \exp[-W(s^2)] ds$$

vanishes as $K^{1/2}$. However, even for the commonly used forms of $W(s^2)$, it is difficult to establish directly that this behavior is possible let alone to find the appropriate variation of h . In fact, for the (unphysical) Gaussian model weighting function, $W(s^2) = a^2 s^2$, one finds²³

$$\begin{aligned} \left(\frac{1}{2}nh\right)^{1-n/2} \int_0^\infty s^{n/2} I_{n/2-1}(nhs) \exp(-a^2 s^2) ds \\ = \frac{1}{2} a^{-n} \exp(n^2 h^2 / 4a^2), \quad (4.17) \end{aligned}$$

which is nonzero for all h . Yet if, for a given weighting function, h can vary in the desired fashion, then the model reduces to the monomer-dimer problem at high temperatures.

The high-temperature series for the quantum-mechanical spin- S Heisenberg model with nearest-neighbor interactions also reduce to the corresponding monomer-dimer expansions at high temperatures. Consider first the standard isotropic interaction $-J\vec{S}_i \cdot \vec{S}_j$, where $\vec{S}_i = (S_i^x, S_i^y, S_i^z)$ is a quantum-mechanical spin operator, associated with the site R_i , which satisfies the usual commutation relations

$$\vec{S}_i \times \vec{S}_i = i\vec{S}_i. \quad (4.18)$$

The partition function in this case is

$$\begin{aligned} Z_N(T, H) = (2S+1)^{-N} \text{Tr} \left[\exp \left(KS^{-2} \sum_{\langle ij \rangle} \vec{S}_i \cdot \vec{S}_j \right. \right. \\ \left. \left. + hS^{-1} \sum_i S_i^z \right) \right], \quad (4.19) \end{aligned}$$

with Tr denoting the trace over all states of the system which are eigenstates of all of the $(\vec{S}_i)^2$ with eigenvalue $S(S+1)$. The factors of S^{-1} and S^{-2} in the exponent and the prefactor $(2S+1)^{-N}$ guarantee the existence of the classical ($S \rightarrow \infty$) limit. The operators $\sum_{\langle ij \rangle} \vec{S}_i \cdot \vec{S}_j$ and $\sum_i S_i^z$ can be shown to commute; as a consequence of this fact and the commutation of spin operators on different sites, Eq. (4.19) becomes

$$\begin{aligned} Z_N(T, H) = (2S+1)^{-N} \text{Tr} \left[\exp \left(KS^{-2} \sum_{\langle ij \rangle} \vec{S}_i \cdot \vec{S}_j \right) \right. \\ \left. \times \prod_i \exp(hS_i^z/S) \right]. \quad (4.20) \end{aligned}$$

It is easy to establish the relation

$$\begin{aligned} \zeta(h, S) &\equiv \text{Tr}[\exp(hS^2/S)] \\ &= \sinh[(S + \frac{1}{2})h/S] / \sinh(h/2S). \quad (4.21) \end{aligned}$$

Then the partition function may be expanded in powers of K to give

$$\begin{aligned} Z_N(T, H) = \left(\frac{\zeta(h, S)}{(2S+1)} \right)^N \sum_{l=0}^{\infty} K^l S^{-2l(l-1)} \\ \times \text{Tr} \left[\left(\sum_{\langle ij \rangle} \vec{S}_i \cdot \vec{S}_j \right)^l \prod_i \left(\frac{\exp(hS_i^z/S)}{\zeta(h, S)} \right) \right]. \quad (4.22) \end{aligned}$$

By multiplying out the l th power of $\sum_{\langle ij \rangle} \vec{S}_i \cdot \vec{S}_j$ one obtains a series which admits a graphical interpretation: in a given term, each factor of $\vec{S}_i \cdot \vec{S}_j$ is represented by the corresponding bond on the lattice. Alternatively, any graph on the lattice (with multiple edges allowed) can be viewed as carrying a weight determined by writing a factor $K \vec{S}_i \cdot \vec{S}_j / S^2$ for each bond, multiplying by $\prod_i [\exp(hS_i^z/S) / \zeta(h, S)]$ and taking the trace over all spins, then averaging over all possible orderings of the bond factors. The trace over any spin not met by any bond gives a factor unity.

We now show that the graphs with l bonds meeting exactly $2l$ magnetic vertices dominate the expansion at high temperature. Such graphs must consist of l single-bond hard dimers, and carry a weight z^l , where

$$\begin{aligned} z &\approx K [S \zeta(h, S)]^{-2} \text{Tr}[\exp(hS_1^z/S) \vec{S}_1 \cdot \vec{S}_2 \exp(hS_2^z/S)] \\ &= K (\partial \ln \zeta / \partial h)^2. \quad (4.23) \end{aligned}$$

By writing this out in explicit form, namely

$$\begin{aligned} z &\approx KS^{-2} \left\{ (S + \frac{1}{2}) \coth[(S + \frac{1}{2})h/S] \right. \\ &\quad \left. - \frac{1}{2} \coth(h/2S) \right\}^2, \quad (4.24) \end{aligned}$$

we see that taking $S \rightarrow \infty$ regenerates the classical result (4.10) for $n=3$ (with nK and nh replaced by K and h). From Eq. (4.23) we see that z can approach a finite value as $K \rightarrow 0$ only if $\partial \ln \zeta / \partial h$ is of order $K^{-1/2}$; since $\zeta(h, S)$ is finite when $\sinh(h/2S) = 0$, this forces h to approach a zero of $\sinh[(S + \frac{1}{2})h/S]$ with corrections of order $K^{1/2}$.

However, graphs of l bonds meeting only $m < 2l$ magnetic vertices, whose weights then contain only m factors of $[\sinh[(S + \frac{1}{2})h/S]]^{-1}$, give contributions which vanish as $K^{l-m/2}$ under these conditions. Thus only the single-bond dimer graphs contribute at high temperatures with fixed z , so that the high-temperature series for this model also reduce to the corresponding monomer-dimer series in this limit. This analysis is still valid (with the form of z unchanged) if the interaction between neighboring spins is of the cylindrically symmetric form

$-J(\alpha S_i^x S_j^x + \alpha S_i^y S_j^y + S_i^z S_j^z)$; specifically, taking $\alpha = 0$ yields the spin- S Ising model.

The above analysis also extends to general interactions $-J\varphi(\vec{S}_i, \vec{S}_j)$ between nearest-neighbor spins. As in the classical n -vector models, "hidden field" terms in φ are allowed, although a condition analogous to Eq. (4.15) must be met. The partition function, given by

$$Z_N(T, H) = (2S + 1)^{-N} \text{Tr} \left[\exp \left(K \sum_{\langle ij \rangle} \varphi(\vec{S}_i, \vec{S}_j) + hS^{-1} \sum_i S_i^z \right) \right], \quad (4.25)$$

can be put in a form resembling Eq. (4.20), despite the fact that the field and interaction parts of the Hamiltonian will not in general commute, by applying the Baker-Campbell-Hausdorff formula,²⁴ which expresses $\ln[\exp(A)\exp(B)]$ for general operators A and B in terms of repeated commutators of A and B . Adopting the notation

$$\{A^n, B\} = [A, \{A^{n-1}, B\}], \quad \text{with } \{A^0, B\} = B, \quad (4.26)$$

this theorem states²⁴

$$\ln[\exp(\lambda A)\exp(\lambda B)] = \sum_{n=1}^{\infty} \lambda^n C_n, \quad (4.27)$$

where the C_n are to be found from

$$\sum_{k=0}^{\infty} [(k+1)!]^{-1} \left\{ \sum_{m=1}^{\infty} \lambda^m C_m \right\}^k, \quad \sum_{n=1}^{\infty} n \lambda^{n-1} C_n \left\{ \right. \\ \left. = A + B + \sum_{j=1}^{\infty} (j!)^{-1} \lambda^j \{A^j, B\} \right\}. \quad (4.28)$$

Setting A equal to the total reduced Hamiltonian and taking $B = -hS^{-1} \sum_i S_i^z$, one finds that the expression (4.25) can be written

$$Z_N(T, H) = (2S + 1)^{-N} \text{Tr} \left[\exp \left(\sum_{m=1}^{\infty} K^m O_m \right) \times \prod_i \exp(hS_i^z/S) \right]. \quad (4.29)$$

The operators O_m arise from multiple commutators involving m factors of $\sum \varphi(\vec{S}_i, \vec{S}_j)$; explicitly we find

$$O_1 = \sum_{\langle ij \rangle} [(l+1)!]^{-1} h^l S^{-l} \{ (S_i^z + S_j^z)^l, \varphi(S_i, S_j) \}, \quad (4.30)$$

and the O_m for $m \geq 2$ will be seen to be unimportant in the high-temperature limit.

Upon expanding the partition function as in Eq. (4.22), the weights of dimer graphs are seen to arise from a dimer activity which is given, for small K , by

$$z \approx K \psi_S(h) / [\zeta(h, S)]^2, \quad (4.31)$$

provided $\psi_S(h)$, defined by

$$\psi_S(h) = \sum_{l=0}^{\infty} [(l+1)!]^{-1} h^l S^{-l} \\ \times \text{Tr} \left\{ \{ (S_1^z + S_2^z)^l, \varphi(\vec{S}_1, \vec{S}_2) \} \exp \left(\frac{h(S_1^z + S_2^z)}{S} \right) \right\}, \quad (4.32)$$

is nonvanishing. If $\psi_S(h)$ is finite (boundedness of φ would guarantee this), then z can remain finite as $K \rightarrow 0$ only if $\zeta(h, S)$ vanishes as $K^{1/2}$, i.e., if h approaches $iS\pi/(S + \frac{1}{2})$ with corrections of order $K^{1/2}$, provided $\psi_S[iS\pi/(S + \frac{1}{2})]$ is nonzero. This latter condition reduces to (4.15) in the classical limit, assuming $\varphi(\vec{S}_1, \vec{S}_2)$ is a function only of the normalized spins \vec{S}_i/S , and means that the single-bond contribution to the free energy does not vanish.

Now if these conditions are met, no contributions arising from the O_m with $m \geq 2$ can survive in the high-temperature limit. Each O_m arises from the m -fold commutator of $\sum \varphi(\vec{S}_i, \vec{S}_j)$ with itself, and so contains terms involving at most $m+1$ spins. Thus it can bring at most $m+1$ factors of $[\zeta(h, S)]^{-1}$ into the weight of any graph. However, O_m carries a factor K^m , and so any term including an O_m with $m \geq 2$ must vanish at least as fast as $K^{(m-1)/2}$ as $K \rightarrow 0$. Finally, the contributions from non-dimer graphs arising only from O_1 terms also vanish in this limit by the same argument used above for the case $\varphi(\vec{S}, \vec{S}') = \vec{S} \cdot \vec{S}'$. Thus for general Heisenberg models, high-temperature series also reduce to the corresponding monomer-dimer expansions at high temperatures.

V. ANALYSIS AND RESULTS

Having established that the dimer density series in the monomer-dimer problem with negative dimer activity describes the high-temperature behavior of the Lee-Yang zero distribution in a wide range of models, we proceed to investigate the position and character of the dominant singularity in $\rho(z)$. The series coefficients ψ_l which determine $\rho(z)$ are known exactly^{9,10} through $l=17$ and $l=14$ for the square and triangular lattices, respectively, and through $l=16$ for the tetrahedral, $l=15$ for the sc, $l=13$ for the bcc, and $l=10$ for the fcc lattices, and are given in Table I. We expect the exponent σ in Eq. (3.12) to lie between the $d=1$ value, $\sigma = -\frac{1}{2}$, and the mean field value, $\sigma = \frac{1}{2}$, which is found for high dimensionalities.⁶ Thus σ could be quite small and difficult to fit. We therefore analyze the series

TABLE I. Coefficients ψ_l of z^l in the dimer density series for various lattices. Coefficients through $l=15$ (square), $l=10$ (triangular), $l=16$ (tetrahedral), $l=12$ (sc), $l=12$ (bcc), and $l=8$ (fcc) are derived from Gaunt (Ref. 9); further coefficients are from Sykes (Ref. 10).

l	square	triangular	tetrahedral
1	2	3	2
2	-14	-33	-14
3	116	432	116
4	-1 042	-6 141	-1 046
5	9 812	91 578	9 932
6	-95 288	-1 409 016	-97 664
7	945 688	22 160 988	984 944
8	-9 537 906	-354 276 333	-10 124 846
9	97 398 764	5 735 254 230	105 646 220
10	-1 004 479 624	-93 777 340 398	-1 115 647 544
11	10 442 811 216	1 545 855 051 480	11 897 857 688
12	-109 291 830 952	-25 654 471 240 104	-127 929 689 312
13	1 150 263 509 280	428 174 286 953 676	1 385 122 530 872
14	-12 164 408 791 920	-7 180 946 872 612 560	-15 086 511 225 632
15	129 177 146 454 536		165 168 901 183 496
16	-1 376 741 271 026 898		-1 816 460 831 076 302
17	14 719 835 348 283 940		

l	simple cubic	body centered	face centered
1	3	4	6
2	-33	-60	-138
3	438	1 096	3 876
4	-6 381	-22 076	-120 126
5	98 298	471 384	3 947 676
6	-1 571 646	-10 462 752	-134 869 584
7	25 804 572	238 712 352	4 736 696 040
8	-432 195 261	-5 559 491 148	-169 820 492 046
9	7 351 521 882	131 557 495 336	6 186 455 616 228
10	-126 601 633 818	-3 152 926 387 520	-228 257 469 246 168
11	2 202 345 302 028	76 350 685 086 240	
12	-38 634 960 958 878	-1 864 887 612 147 680	
13	682 589 371 293 612	45 882 795 957 148 336	
14	-12 133 302 712 160 964		
15	216 812 614 019 536 368		

for the susceptibility / dimer compressibility

$$\chi(z) = \frac{d\rho(z)}{dz}, \quad (5.1)$$

which must then have a stronger singularity than $\rho(z)$, namely

$$\chi(z) \sim (z + z_0)^{\sigma-1}, \quad \text{for } z \rightarrow -z_0. \quad (5.2)$$

Since the constant term in each of the $\rho(z)$ series is zero, no coefficients are lost in this differentiation.

Ratio analysis¹⁹ of these series yields estimates for the singularity position z_0 and the exponent σ which are shown in Table II. We expect σ to have the

same value in both two-dimensional lattices and in all of the three-dimensional lattices; this is not inconsistent with the results and leads to the overall estimates⁶

$$\begin{aligned} \sigma &= -0.155 \pm 10, \quad \text{for } d = 2, \\ \sigma &= 0.098 \pm 12, \quad \text{for } d = 3, \end{aligned} \quad (5.3)$$

with uncertainties covering the spread in the estimates of σ for lattices of the same dimensionality. The ratio test and Padé approximant methods were applied to these series by Gaunt,⁹ although fewer terms were then available. His estimates for the

TABLE II. Estimates, \bar{z}_0 , of the position of the singularity, $z = -z_0$, and $\bar{\sigma}$, of the exponent σ , from various studies of the monomer-dimer compressibility series for several lattices. Gaunt's results (Ref. 9) were obtained from shorter series than are now available. As explained in the text, the current ratio estimates (central column and Ref. 6) are considered less reliable, owing to the severe curvature of the ratio plots, than the estimates based primarily on the inhomogeneous differential approximants (and recursion relation analyses) as illustrated in Figs. 1 and 2.

lattice		Gaunt	ratio (present)	overall (present)
square	\bar{z}_0	0.08895_{-2}^{+5}	$0.08895_2 \pm 2$	0.088963 ± 2
	$\bar{\sigma}$		-0.159 ± 14	-0.1645 ± 20
triangular	\bar{z}_0	0.05600 ± 10	0.056060 ± 6	0.056076 ± 2
	$\bar{\sigma}$		-0.153 ± 6	-0.1620 ± 15
tetrahedral	\bar{z}_0	0.08500_{-3}^{+4}	0.084959 ± 11	0.085015 ± 15
	$\bar{\sigma}$		0.090 ± 6	0.070 ± 15
simple cubic	\bar{z}_0	0.05200 ± 6	0.052002 ± 6	0.052025 ± 5
	$\bar{\sigma}$		0.096 ± 6	0.081 ± 6
body centered	\bar{z}_0	0.03730_{-5}^{+4}	0.037294 ± 14	0.037309 ± 4
	$\bar{\sigma}$		0.103 ± 10	0.090 ± 5
face centered	\bar{z}_0	0.02420 ± 10	0.024213 ± 18	0.024224 ± 6
	$\bar{\sigma}$		0.109 ± 17	0.097 ± 11

singularity position are displayed in Table II; no values for σ were quoted. The present estimates of z_0 are consistent with those of Gaunt and are more precise. However, an appreciable curvature in the dependence of the l th ratio on l^{-1} makes extrapolation difficult and suggests that the form

$$\chi(z) \approx A(z)(z + z_0)^{\sigma-1}, \quad \text{for } z \approx -z_0, \quad (5.4)$$

with $A(z)$ analytic and finite at $-z_0$, may not be sufficient to describe the asymptotic behavior of $\chi(z)$.

Fitting Padé approximants to the logarithmic derivative of the function under consideration²⁵ has proven quite successful for analyzing algebraic singularities such as Eq. (5.4). We have applied this technique to the series for $\chi(z)$; the estimates \bar{z}_0 , for z_0 , and $\bar{\sigma}$, for σ , obtained for the square and sc lattices, which are typical of the results for two- and three-dimensional lattices, respectively, are plotted as open circles in Figs. 1 and 2. The correlation between \bar{z}_0 and $\bar{\sigma}$ is quite strong and shows very little scatter, but the results converge rather slowly as the number of terms used in calculating the approximants is increased. The apparent limits of the sequences of \bar{z}_0 values differ from the ratio estimates, although they fall within the ranges given by Gaunt. Furthermore, the estimates $\bar{\sigma}$ seem to converge to values which disagree with the ratio estimates and with the apparent limits for other lattices of the same dimensionality.

In order to obtain more estimates of z_0 and σ , we have also applied the Dlog Padé technique to the

series for

$$(z\chi)' = \frac{d[z\chi(z)]}{dz}, \quad (5.5)$$

whose behavior is near $-z_0$ is given by

$$[z\chi(z)]' \sim (z + z_0)^{\sigma-2}, \quad \text{for } z \rightarrow z_0. \quad (5.6)$$

The estimates obtained in this manner for the square and simple cubic lattices are plotted as crosses in Figs. 1 and 2. The trends followed by these estimates are consistent with the apparent limits of the \bar{z}_0 and $\bar{\sigma}$ sequences obtained from Dlog approximants to $\chi(z)$. The approximants for $\chi(z)$ and $(z\chi)'$ tended to place sequences of pole-zero pairs along the negative real z axis to the left of $-z_0$, beginning within about 10% of $-z_0$, which suggests that they may be trying to fit a branch cut. This provides further evidence that Eq. (5.4) must be generalized in order to adequately represent $\chi(z)$ for z near $-z_0$.

In order to obtain refined estimates of σ we have formed Padé approximants to the function $(z + \bar{z}_0) d[\log\chi(z)]/dz$ and evaluated the approximants at $z = -\bar{z}_0$, using \bar{z}_0 as an input parameter. If the exact value of z_0 is used, this function takes on the value $\sigma - 1$ at $z = -z_0$. For each lattice a range of values of \bar{z}_0 around the apparent limit of the Dlog Padé estimates was used. The results for the square and sc lattices are plotted as solid lines in Figs. 1 and 2. Clearly the values of $\bar{\sigma}$ thus obtained depend strongly on the specified \bar{z}_0 , with the dependence following closely the correlation which arises from the

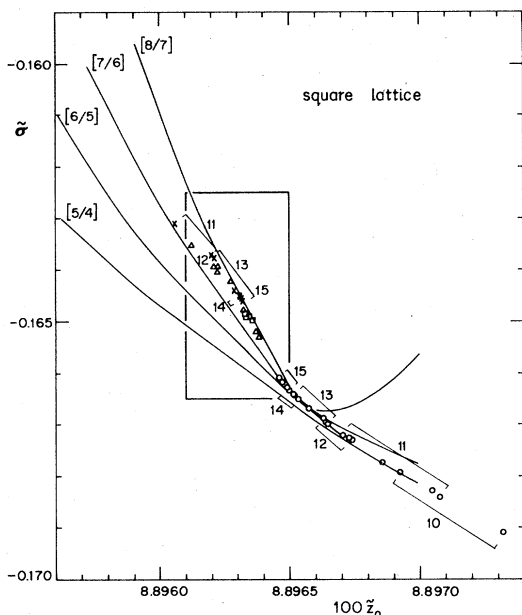


FIG. 1. Estimates obtained from analysis of the dimer density series on the square lattice. Open circles mark the estimated singularity position $-\bar{z}_0$ and exponent σ given by Padé approximants to the indicated number of terms in the series expansion of $d \ln \chi(z)/dz$; crosses are from Padé approximants to $d \ln [z \chi(z)]'/dz$. Solid lines are the results of Padé approximants to $(z + \bar{z}_0) d \ln \chi(z)/dz$ with \bar{z}_0 given as an input parameter. Squares indicate points obtained from inhomogeneous Dlog Padé approximants to $\chi(z)$ and $[z \chi(z)]'$, and triangles locate estimates provided by the recursion-relation method. The "error box" corresponds to the best estimates quoted in Table II.

unbiased methods.

The inhomogeneous differential approximant, or UPQ approximant, method^{12,13} is designed to analyze singularities which are superimposed on an analytic background, and so could fit the form

$$\chi(z) \approx A(z)(z + z_0)^{\sigma-1} + B(z), \quad \text{for } z \approx -z_0, \quad (5.7)$$

where $A(z)$ and $B(z)$ are finite and smooth at $z = -z_0$. We have tested this method on the dimer density series for the Bethe lattice with coordination number q , whose singularity is known exactly^{4,8} to be given by $\sigma = \frac{1}{2}$. Dlog Padé approximants to the first seventeen terms of the series for $q = 4$ and $q = 12$ can only come within 25% of the correct value of σ . The $[J/L; M]$ UPQ approximants with $L < 2$ or $M < 3$ do no better than the Dlog Padé approximants, but all those we have calculated with $L \geq 2$ and $M \geq 3$ give excellent estimates for σ , falling within a few parts in 10^4 of the exact value for $q = 4$ and within parts in 10^6 for $q = 12$. In fact, the singularity is reproduced exactly by a $[0/2; 3]$ approximant. Clearly the pole which lies on the second Riemann

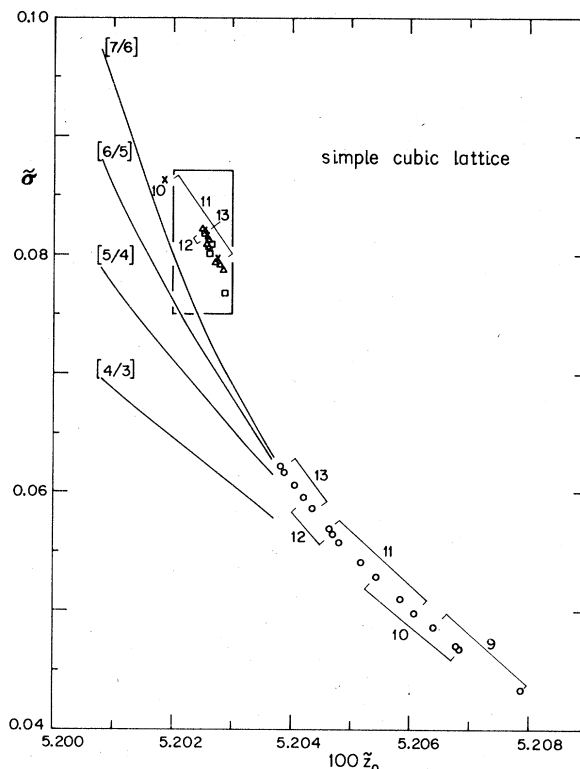


FIG. 2. Estimates for the simple cubic lattice, as in Fig. 1.

sheet of the dimer density function,⁴ and which slows the convergence of Padé approximants, fails to deceive the UPQ approximants. The nonoccurrence of singular matrices in the calculation of the longer approximants is indeed remarkable, and points out the present lack of understanding of the uniqueness problem for UPQ approximants.

For the square and sc lattices, the estimates for z_0 and σ obtained from UPQ approximants with $J \geq 1$ and $\chi(z)$ and $(z\chi)'$ are displayed as squares in Figs. 1 and 2. The values of \bar{z}_0 and $\bar{\sigma}$ taken from these approximants fall near the estimates obtained from the other methods described above and are much more consistent for each lattice; furthermore, the values of the backgrounds at $-\bar{z}_0$ and the positions of the second singularities along the negative real axis are fairly consistent for the "diagonal" $[J/L; L]$ and $[J/L; L \pm 1]$ approximants. The UPQ approximants can also be biased to force a singularity to occur at a specified position $-\bar{z}_0$, thus yielding refined estimates for σ . The estimates obtained in this manner are consistent with the above results.

The recursion relation method¹¹ is capable of resolving confluent power-law singularities,

$$\chi(z) \approx A(z)(z + z_0)^{\sigma-1} + B(z)(z + z_0)^{\phi-1} \quad \text{for } z \approx -z_0, \quad (5.8)$$

with $\sigma < \phi$. The method can also be modified to in-

clude an analytic background term $C(z)$ in Eq. (5.8). However, when applied to the present series, it produces no evidence of confluence, but reconfirms the estimates of z_0 and σ obtained from the other methods. The estimates obtained from the series for the square and simple cubic lattices are plotted as triangles in Figs. 1 and 2, and can be seen to be almost as consistent as the estimates taken from *UPQ* approximants. The recursion relation method can also be biased to force a singularity at any desired location; using this technique to obtain refined estimates of σ yields estimates which are consistent with the overall pictures emerging from the results of the other approximation methods.

Our final estimates of z_0 and σ for the various lattices, taken mainly from the *UPQ* approximant and recursion relation analysis, are listed in Table II. Owing to the curvature in the ratio plots for these series, we expect these estimates to be more reliable than those obtained from ratio analysis. On the assumption that σ is independent of details of lattice structure for a given dimensionality, we conclude

$$\begin{aligned} \sigma &= -0.163 \pm 3, \quad \text{for } d=2, \\ \sigma &= 0.086 \pm 15, \quad \text{for } d=3. \end{aligned} \quad (5.9)$$

The differences among the estimates of σ obtained for different lattices of the same dimensionality suggest that the apparent consistency and convergence of the estimates for any one lattice are somewhat misleading. A similar situation arises in most other lattice extrapolation problems, although with series as long as available here the spread of exponent estimates is often smaller. One possible cause of slow convergence is the presence of confluent singularities; however, the recursion relation method gave little positive indication of their presence. Nevertheless, the apparently better behavior of the differential or *UPQ* approximants and the recursion relation technique suggests that background terms and confluent or close-by singularities are playing a larger role than in some other lattice problems.

VI. DISCUSSION

We have shown that the nature of the singularity in the density of Lee-Yang zeros at the edge of the zero distribution in n -vector models with nearest-neighbor interactions is independent of n at high temperatures. This may not be so surprising, since⁶ the magnetic field present at the edge breaks the symmetry of the problem in spin space, leading to Ising-like ($n=1$) behavior near the singularity. More remarkable, perhaps, is the fact that the form of the zero density in this limit can explicitly be demonstrated to be independent of the quantal or classical na-

ture of the spins and of the detailed form of the interactions between spins, and seems to depend only on the fact that the interactions link nearest-neighbor spins.

In fact we expect the universality of the exponent σ to persist for all temperatures above critical, although the symmetry of the model may affect the behavior of the amplitude of the singularity and must enter into the position of the Yang-Lee edge near $T=T_c$. The temperature independence of σ for temperatures not too close to T_c has been checked numerically for Ising models on the square and tetrahedral lattices by Kortman and Griffiths,⁵ although high precision was not possible. The n independence of σ accords with renormalization-group analysis,⁶ and with numerical work¹⁷ based on transfer integral methods for one-dimensional systems, which likewise indicate that σ is independent of temperature for temperatures above critical. It is clear that this n independence does not extend to the infinite- n limit, since the Yang-Lee edge singularity in spherical models is given by⁷ $\sigma = \frac{1}{2}$ for all d . Understanding this nonuniformity of the infinite- n

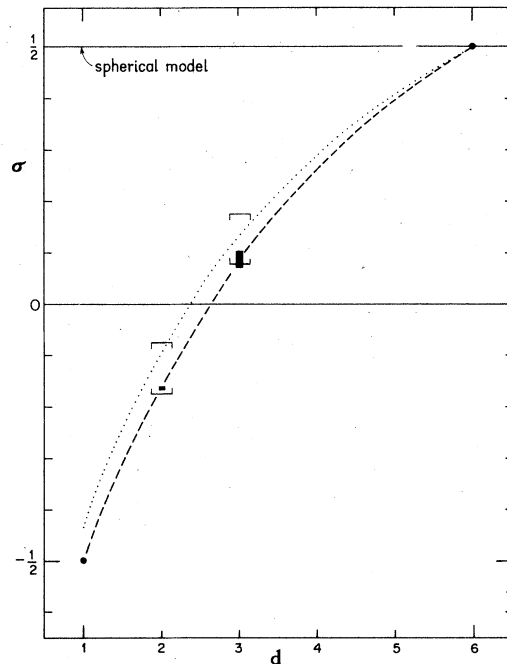


FIG. 3. Dependence of the exponent σ on dimensionality d . For $d > 6$, σ maintains the value $+\frac{1}{2}$; for the spherical model $\sigma = +\frac{1}{2}$ for all d . Solid bars mark the present estimates, while open error limits locate those of Kortman and Griffiths. Lines are taken from renormalization-group analysis, with σ given by the hyperscaling relation (6.1), and with η given by the [1/1] (dotted line) and [2/1] (dashed line) two-point Padé approximants in Eq. (6.4). The point ($d=1, \sigma=-\frac{1}{2}$) is exact (Ref. 6).

limit requires further study.

The estimates of σ obtained here are more precise but fall within the ranges proposed by Kortman and Griffiths⁵ in their original work. Renormalization-group analysis⁶ predicts that for $d \leq 6$ the exponent σ is related to the exponent η for the scaling decay of the basic two-point correlation function at the Yang-Lee edge by

$$\sigma = (d - 2 + \eta)/(d + 2 - \eta) . \quad (6.1)$$

The estimates (5.9) then correspond to

$$\begin{aligned} \eta &= -0.78 \pm 2 , \quad \text{for } d = 2 , \\ \eta &= -0.52 \pm 8 , \quad \text{for } d = 3 . \end{aligned} \quad (6.2)$$

An expansion for small positive $\epsilon = 6 - d$ leads to⁶

$$\eta = -\frac{1}{9}\epsilon - \frac{43}{729}\epsilon^2 + O(\epsilon^3) . \quad (6.3)$$

Forming two-point [1/1] and [2/1] Padé approximants to this, together with the exact result $\eta = -1$ for $d = 1$, yields respectively

$$\eta \simeq -5\epsilon/(45 - 4\epsilon) \quad (6.4a)$$

and

$$\eta \simeq -\epsilon(180 + 179\epsilon)/(1620 + 751\epsilon) . \quad (6.4b)$$

The corresponding continuous variation of σ with d is plotted in Fig. 3 along with our best estimates and those of Kortman and Griffiths; the [2/1] approximant in Eq. (6.4b) leads to

$$\begin{aligned} \sigma &\simeq -0.1623 , \quad \text{for } d = 2 , \\ \sigma &\simeq 0.0800 , \quad \text{for } d = 3 , \end{aligned} \quad (6.5)$$

which compare very favorably with the estimates (5.9).

ACKNOWLEDGMENTS

We wish to thank Dr. M. F. Sykes for sending us his unpublished data, and Dr. P. Moussa and Dr. G. A. Baker, Jr. for helpful criticisms and suggestions. The support of the NSF, in part through the Materials Science Center at Cornell University, is gratefully acknowledged. M.E.F. is indebted to the John Simon Guggenheim Memorial Foundation for a Fellowship Award. Dr. Helen Au-Yang kindly assisted in deriving the data presented in Table I.

¹C. N. Yang and T. D. Lee, Phys. Rev. **87**, 404 (1952).

²T. D. Lee and C. N. Yang, Phys. Rev. **87**, 410 (1952).

³G. Gallavotti, S. Miracle-Solé, and D. W. Robinson, Phys. Lett. A **25**, 493 (1967).

⁴J. D. Bessis, J. M. Drouffe, and P. Moussa, J. Phys. A **9**, 2105 (1976).

⁵P. J. Kortman and R. B. Griffiths, Phys. Rev. Lett. **27**, 1439 (1971).

⁶M. E. Fisher, Phys. Rev. Lett. **40**, 1610 (1978).

⁷D. A. Kurtze and M. E. Fisher, J. Stat. Phys. **19**, 205 (1978).

⁸G. A. Baker, Jr. and P. Moussa, J. Appl. Phys. **49**, 1360 (1978).

⁹D. S. Gaunt, Phys. Rev. **179**, 174 (1969). This paper contains further references to the monomer-dimer problem.

¹⁰M. F. Sykes (unpublished).

¹¹A. J. Guttmann and G. S. Joyce, J. Phys. A **5**, L81 (1972).

¹²M. E. Fisher and H. Au-Yang, J. Phys. A (to be published)

¹³G. A. Baker, Jr. and D. L. Hunter, Phys. Rev. B **19**, 3808 (1979).

¹⁴T. Asano, J. Phys. Soc. Jpn. **29**, 350 (1970), and Phys. Rev. Lett. **24**, 1409 (1970).

¹⁵M. Suzuki and M. E. Fisher, J. Math. Phys. **12**, 235 (1971).

¹⁶F. Dunlop and C. M. Newman, Commun. Math. Phys. **44**, 223 (1975).

¹⁷D. A. Kurtze, Ph.D. thesis (Cornell University, 1979) (unpublished).

¹⁸E. Byckling, Phys. Rev. **140**, A1165 (1965).

¹⁹See, e.g., M. E. Fisher, Rep. Prog. Phys. **30**, 615 (1967).

²⁰See, e.g., C. Domb, in *Phase Transitions and Critical Phenomena*, edited by C. Domb and M. S. Green (Academic, New York, 1974), Vol. 3, p. 357.

²¹H. E. Stanley, Phys. Rev. **176**, 718 (1968).

²²M. Kac and C. J. Thompson, Phys. Norv. **5**, 163 (1971).

²³A. Erdélyi, et al., *Higher Transcendental Functions* (McGraw-Hill, New York, 1953), Vol. 2, p. 232.

²⁴See R. M. Wilcox, J. Math. Phys. **8**, 962 (1967).

²⁵G. A. Baker, Jr., Phys. Rev. **124**, 768 (1961).